The Effect of Convective Response Time on WISHE Modes

KERRY EMANUEL

Center for Meteorology and Physical Oceanography, Massachusetts Institute of Technology, Cambridge, Massachusetts

(Manuscript received 6 April 1992, in final form 21 September 1992)

ABSTRACT

Recent research has shown that a variety of wavelike oscillations in the tropics may be explained by instabilities driven by wind-induced surface heat exchange (WISHE). All such studies to date have implicitly assumed that moist convection is in quasi equilibrium with the flow in question. Here that assumption is relaxed by accounting for a small but nonzero lag between the large-scale forcing of convection and its response. Reaction times as short as 30 minutes damp the higher-frequency Kelvin-like equatorial modes, favoring zonal wavenumbers 1–4, and strongly bias the higher-order modes to westward-propagating disturbances of synoptic scale. An analysis of off-equatorial disturbances reveals a preference for poleward- and westward-propagating modes with wavelengths of the order of 1000 km.

1. Introduction

It has generally been assumed that the latent heat released in cumulus clouds is the main energy source for many tropical disturbances. Historically, this view probably arose from the circumstance that convective clouds were first studied intensively in North America, where the particular geography allows for the accumulation of large quantities of convective available potential energy (CAPE). It was natural to assume that this was so in the tropics as well, though the average amount of CAPE is somewhat less. For many decades, the origin of tropical disturbances was regarded as a problem of determining the mechanism by which this energy could be used to drive the circulations. Among the most prominent theories of this kind is conditional instability of the second kind (CISK), originally developed by Charney and Eliassen (1964) and Ooyama (1964) in an attempt to explain the origin of tropical cyclones. In essence, CISK works by selectively releasing CAPE in regions where the large-scale circulation happens to converge water vapor, repressing it elsewhere.

There is increasing evidence that such a view is mistaken. In the first place, careful analysis of maritime tropical soundings casts doubt on the existence of a reservoir of CAPE (Betts 1982; Xu and Emanuel 1989). A more recent study by Randall and Wang (1992) indicates that only a very small fraction of the subcloud layer can convect before all of the available potential energy of the atmosphere is used up. Even more compelling is the observation by Arakawa and Schubert (1974) that the rate of change of CAPE in the maritime tropical atmosphere is very much smaller than what would occur if the destabilization of the atmosphere by large-scale processes were unopposed by convection. This shows that the temperature of the convecting atmosphere (and thus its mass distribution) is determined by the condition that convection is in statistical equilibrium with the large scale, and not by the selective release of stored CAPE.

Compared to the small and perhaps nonexistent reservoir of CAPE in the maritime tropics, the amount of realizable energy represented by the thermodynamic disequilibrium between the tropical oceans and atmosphere is huge. This is the energy source for hurricanes, as first pointed out by Kleinschmidt (1951) and demonstrated quantitatively by Emanuel (1986). It is natural to suppose that this large reservoir of energy is also active in other types of tropical circulations. One way of realizing this energy source is through the wind dependence of the rate of transfer of enthalpy from the ocean to the atmosphere, as is the case in hurricanes. This mechanism has been called wind–evaporation feedback by Neelin et al. (1987) and wind-induced surface heat exchange (WISHE) by Yano and Emanuel (1991), who wished to emphasize that, in principle, the mechanism can work on the exchange of sensible as well as latent heat.

The WISHE mechanism was proposed as an explanation of the 30–50-day oscillation by Neelin et al. (1987) and Emanuel (1987). They showed that the enhancement of the mean surface easterlies ahead of an eastward-propagating trough leads to enhanced transfer of enthalpy from the ocean and associated warming of the troposphere when this enthalpy increase is distributed through the troposphere by convection. In addition to this Kelvin-like mode, higher-frequency

Corresponding author address: Dr. Kerry A. Emanuel, Center for Meteorology and Physical Oceanography, Massachusetts Institute of Technology, Cambridge, MA 02139.

eastward- and westward-propagating modes were found by Emanuel (1987). Goswami and Goswami (1991) have proposed that some of these may be associated with observed westward-propagating disturbances over the western Pacific.

All of the aforementioned studies have assumed that convection is in statistical equilibrium with the resolved flow. Emanuel (1987) assumed further that the precipitation efficiency of the convection was 100% so that no downdrafts are formed and the boundary-layer enthalpy is essentially unaffected by the convection. This leads to the result that adiabatic cooling in ascent regions is completely compensated by convective heating, so that perturbations onto a convecting atmosphere feel no bulk stratification. Yano and Emanuel (1991) relaxed this restriction by allowing for downdrafts, and showed that this causes the disturbances to feel a net stratification that varies as the dry stratification multiplied by one minus the precipitation efficiency. Earlier, Neelin et al. (1987) had used a small net stable stratification justified by a different but consistent line of reasoning. The importance of downdrafts was emphasized as well by Emanuel (1989), who presented evidence that they prevent weak tropical disturbances from becoming hurricanes. It seems probable that a reasonable description of the dynamics of convecting atmospheres must take into account the stabilizing effects of convective downdrafts.

Comparison of the linear WISHE modes with observations reveals some disturbing attributes of the former. The eastward-propagating Kelvin-like mode has its maximum growth rate at small scales, whereas the observed phenomenon is of planetary scale. Moreover, the higher-order modes discussed by Emanuel (1987) and more extensively by Goswami and Goswami (1991) show a strong preference for small-scale, eastward-propagating waves, although westward-propagating modes are allowed. Yano and Emanuel (1991) showed that the shorter, Kelvin-like waves are strongly damped by upward propagation into the stratosphere, providing a planetary-scale bias for these modes.

The purpose of the present work is to demonstrate that the relaxation of the quasi-equilibrium assumption, by allowing for a small response time of convection to the large-scale forcing, strongly damps the high-frequency WISHE modes, leaving intact essentially three classes of unstable disturbances: equatorially trapped long-wave Kelvin-like modes and synoptic-scale westward-propagating $n = 0$ modes, and poleward- and westward-propagating modal disturbances that are not necessarily confined to the equatorial zone. The linear equations are developed in section 2, while solutions of these are presented in section 3. Section 4 provides a summary.

2. The linear model

We begin with the linear equations used by Yano and Emanuel (1991, hereafter YE). These represent the linearization of the primitive equations on an equatorial beta plane, with the mean state consisting of a constant easterly wind in an atmosphere considered to be in radiative–convective equilibrium. Here, for simplicity, we drop all the damping terms. Following Emanuel (1987) and YE, the atmosphere is always considered to have a moist adiabatic temperature lapse rate representing a saturation θ_e equal to the actual θ_e of the boundary layer, and only the first baroclinic mode is considered in the vertical structure. (The higher modes are forbidden by the assumption of the moist adiabatic lapse rate). We also neglect upward radiation of wave energy into the stratosphere. With these assumptions, there is a strict relation between fluctuations of the geopotential of the boundary layer and fluctuations of subcloud-layer moist entropy, given by

$$\delta\phi_b = -C_p T_b \bar{\epsilon}\, \delta(\ln\theta_{eb}), \tag{1}$$

where C_p is the heat capacity at constant pressure, T_b is the mean subcloud-layer temperature, θ_{eb} is the subcloud-layer equivalent potential temperature, and $\bar{\epsilon}$ is given by

$$\bar{\epsilon} \equiv (T_b - \bar{T})/T_b, \tag{2}$$

where $\bar{T}$ is the mass-weighted tropospheric mean temperature. (See Emanuel 1987 for a complete derivation of this.)

Note that (1), which is a crucial feature of models of this kind, is another way of expressing the quasi-equilibrium hypothesis of Arakawa and Schubert (1974). The only way for the convective available potential energy of the atmosphere to remain constant is for the entropy (θ_e) of the boundary layer to change in concert with the mean virtual temperature of the free atmosphere. This vertically integrated virtual temperature is in turn related to the geopotential through the hydrostatic condition. While measurements of θ_e in the tropics are not good enough to verify (1) directly for observed amplitudes of $\delta\phi_b$, the quasi-equilibrium hypothesis has been confirmed against observations rather thoroughly (e.g., Arakawa and Schubert 1974, 693–694).

The linear equations for subcloud-layer zonal and meridional wind, mass continuity, tropospheric temperature, and subcloud-layer entropy are

$$\left(\frac{\partial}{\partial t} + \bar{U}\frac{\partial}{\partial x}\right)u = -\frac{\partial\phi}{\partial x} + \beta y v, \tag{3}$$

$$\left(\frac{\partial}{\partial t} + \bar{U}\frac{\partial}{\partial x}\right)v = -\frac{\partial\phi}{\partial y} - \beta y u, \tag{4}$$

$$\frac{\partial u}{\partial x} + \frac{\partial v}{\partial y} + \frac{1}{H_m}(M_c + M_d) = 0, \tag{5}$$

$$g\left(\frac{\partial}{\partial t} + \bar{U}\frac{\partial}{\partial x}\right)\ln\theta = -N^2 M_d, \tag{6}$$

$$h\left(\frac{\partial}{\partial t}+\bar{U}\frac{\partial}{\partial x}\right)\ln\theta_{eb}=C_\theta\ln\frac{\theta_{es}}{\bar{\theta}_{eb}}\,\mathrm{sgn}(\bar{U})u+\frac{N^2H}{g}(\epsilon_pM_d-(1-\epsilon_p)M_c),\quad(7)$$

where $\bar{U}$ is the mean zonal wind, u and v are the subcloud-layer zonal and meridional wind perturbations, ϕ is the boundary-layer geopotential perturbation, β is the meridional gradient of the Coriolis parameter at the equator, M_c is the mass flux in convective clouds, M_d the mass flux outside of convective clouds, θ the average tropospheric potential temperature, g the acceleration of gravity, N the buoyancy frequency of dry air, H the thickness of the troposphere, H_m the altitude of the entropy minimum, h the thickness of the subcloud layer, C_θ the bulk surface heat exchange coefficient, ϵ_p the bulk precipitation efficiency, θ_{es} the saturation entropy of the ocean surface, and θ_{eb} is the θ_e of the subcloud layer. In addition, the total vertical velocity is given by

$$w=M_c+M_d.\quad(8)$$

Finally, there is a relationship between fluctuations of saturation entropy and of dry entropy (see Emanuel 1987):

$$\delta\ln\theta=(\Gamma_m/\Gamma_d)\delta\ln\theta_e^*=(\Gamma_m/\Gamma_d)\delta\ln\theta_{eb},\quad(9)$$

where θ_e^* is the saturation entropy, Γ_m and Γ_d are the moist and dry adiabatic lapse rates, respectively, and we have made use of the condition of moist neutrality.

The scaling relations developed by YE show that, having dropped the damping terms, it is necessary to also drop the left-hand side of (7) to be consistent. This amounts to a quasi-equilibrium condition on the subcloud-layer entropy, holding that the fluxes of entropy from the sea surface are balanced by fluxes through the top of the subcloud layer. (We stress that this is a *quasi*-balance assumption; it does not imply that there are no changes in subcloud-layer θ_e, for this would negate all the physics of this model.) Neglecting the left-hand side of (7) and using (8) to eliminate M_d yields a diagnostic relation for the cumulus mass flux:

$$M_c=\epsilon_pw+\frac{g}{N^2H}C_\theta\ln\frac{\theta_{es}}{\bar{\theta}_{eb}}\,\mathrm{sgn}(\bar{U})u.\quad(10)$$

This shows that anomalies of the convective updraft mass flux are forced by anomalies in the large-scale ascent and by anomalies in the surface enthalpy flux due to fluctuations of the zonal wind.

It is at this point that we introduce a time lag between the forcing of convection and its response. Physically, this may be regarded as a consequence of the time it takes for clouds to form and precipitation to fall, including perhaps the time scales associated with mesoscale processes such as anvil formation and production of precipitation. It is obviously not our purpose to produce a detailed representation of these effects, but only to demonstrate that they have important effects on WISHE modes. In keeping with the simplicity of this model, we merely introduce a time lag between the forcing of convection and its response; the right-hand side of (10) is therefore evaluated with a time lag:

$$M_c=\left[\epsilon_pw+\frac{g}{N^2H}C_\theta\ln\frac{\theta_{es}}{\bar{\theta}_{eb}}\,\mathrm{sgn}(\bar{U})u\right]\Bigg|_{t=t-\tau},\quad(11)$$

where τ is the time lag. Observations suggest that this time scale is of the order of 20 minutes to several hours (Betts and Miller 1986).

It is instructive to see how this affects the response of temperature to large-scale ascent and to surface fluxes. We first substitute (9) into the temperature equation (6) to express the latter in terms of subcloud-layer entropy. We then use (8) to express M_d in terms of w and M_c, and (11) for M_c. The result is

$$g\left(\frac{\partial}{\partial t}+\bar{U}\frac{\partial}{\partial x}\right)\ln\theta_{eb}=-\frac{\Gamma_d}{\Gamma_m}N^2(w-\epsilon_pw|_{t=t-\tau})+\frac{\Gamma_d}{\Gamma_m}\frac{g}{H}C_\theta\ln\frac{\theta_{es}}{\theta_{eb}}\,\mathrm{sgn}(\bar{U})u\Bigg|_{t=t-\tau}.\quad(12)$$

First, consider the case of $\tau=0$. When the precipitation efficiency ϵ_p is unity, large-scale vertical motion does not affect the boundary-layer entropy by exciting downdrafts, since the latter are not possible. In effect, the boundary-layer processes control the free atmosphere temperature. This was the case considered by Emanuel (1987). At the opposite extreme, when $\epsilon_p=0$, there can be no net heating by moist convection and the boundary-layer entropy is forced by shallow convection to track changes in free atmosphere temperature, which in turn result from adiabatic warming and cooling by the large-scale flow. The second term on the right-hand side of (12) represents the effect of anomalous surface fluxes of enthalpy on atmospheric temperature, given that moist convection always distributes these changes aloft.

If the response time τ is not zero, then both the convective effects on the stratification and on distributing the surface fluxes aloft are lagged.

We now look for modal solutions of the form

$$e^{ikx+\sigma t},$$

where σ is a complex growth rate. We nondimensionalize the dependent and independent variables as well as the mean zonal wind $\bar{U}$ according to the scaling given in Table 1, which also gives typical values of the scaling parameters. In addition, we use (1) to eliminate the geopotential. We also assume hereafter that the background zonal wind is from the east. The resulting set, derived from (3)–(5), (8), and (12) is

$$Du=ikT+vy,\quad(13)$$

TABLE 1. Scaling parameters.

Variable	Scaling factor (see definitions below)	Typical value
x	HF/A	7000 km
y	$(\Gamma FB)^{1/4}\beta^{-1/2}$	1500 km
t	$(F/\Gamma B)^{1/2}H/A$	1.6 d
u	$F(HB/aA)^{1/2}$	40 m s^{-1}
v	$(A/a\beta H)^{1/2}(\Gamma FB^3)^{1/4}$	8 m s^{-1}
w, M_c, M_d	$H_m(AB/Ha)^{1/2}$	4 cm s^{-1}
ϕ	$B(\Gamma HF^3/aA)^{1/2}$	2000 m^2 s^{-2}
$\ln\theta_{eb}$	$(\Gamma HF^3/aA)^{1/2}$	0.07
U	$(\Gamma FB)^{1/2}$	50 m s^{-1}

Definitions: $A \equiv C_\theta \ln(\theta_{es}/\bar{\theta}_{eb})$, $B \equiv \bar{\epsilon}C_pT_b$, $F \equiv N^2H_m/g$, $\Gamma \equiv \Gamma_d/\Gamma_m$, $a \equiv$ radius of earth.

$$Dv = P\left[\frac{dT}{dy} - yu\right], \tag{14}$$

$$iku + \frac{dv}{dy} + w = 0, \tag{15}$$

$$DT = -w(1 - \epsilon_p e^{-\sigma\tau}) + ue^{-\sigma\tau}, \tag{16}$$

where

$$D \equiv \sigma + ikU$$

$$P \equiv \beta\left(\frac{N^2H_m}{g}\right)^{3/2}\left(C_\theta \ln\frac{\theta_{es}}{\bar{\theta}_{eb}}\right)^{-2} \times H^2\left(\frac{\Gamma_d}{\Gamma_m}\bar{\epsilon}C_pT_b\right)^{-1/2} \approx 25. \tag{17}$$

In the above, T is the scaled version of $\ln(\theta_{eb})$. Note that aside from the factor $e^{-\sigma\tau}$ these equations are identical to those used by Neelin et al. (1987), YE, and Goswami and Goswami (1991). They may be combined into a single equation in v:

$$\frac{d^2v}{dy^2} - \frac{1}{\sigma\chi}y\frac{dv}{dy} - v\left[\frac{1}{P\chi}(\sigma^2 + k^2\chi^2 + ike^{-\sigma\tau}) + \frac{y^2}{\chi} + \frac{1}{\sigma\chi} - \frac{ik}{\sigma}\right] = 0, \tag{18}$$

where

$$\chi \equiv 1 - \epsilon_p e^{-\sigma\tau}.$$

By making the transformation

$$v = v' \exp\left[\frac{y^2}{4\sigma\chi}\right],$$

(18) may be transformed into the standard form

$$\frac{d^2v'}{dy^2} - v'\left[y^2\left(\frac{1}{\chi} + \frac{1}{4}\frac{e^{-2\sigma\tau}}{\sigma^2\chi^2}\right) + \frac{1}{P\chi} \times (\sigma^2 + \chi k^2 + ike^{-\sigma\tau}) + \frac{1}{2}\frac{e^{-\sigma\tau}}{\sigma\chi} - \frac{ik}{\sigma}\right] = 0. \tag{19}$$

Provided that we demand that $v \to 0$ as $y^2 \to \infty$, (19) has standard solutions in terms of parabolic cylinder functions. This entails the eigenvalue relation

$$ik\chi - \frac{1}{2}e^{-\sigma\tau} - \frac{\sigma}{P}(\sigma^2 + \chi k^2 + ike^{-\sigma\tau}) = \pm(2n + 1)\left(\chi\sigma^2 + \frac{1}{4}e^{-2\sigma\tau}\right)^{1/2}, \tag{20}$$

where n is an integer.

It can be seen that were it not for the exponent terms in (20), it would be a sixth-order equation for the complex growth rate σ. If the time lag τ is very small compared to the time scales of the disturbances we are interested in and we expand the exponent to first order:

$$e^{-\sigma\tau} \approx 1 - \sigma\tau,$$

the order of the equation does not change: it is still sixth order. In general, however, the exponent terms will yield more roots than the six that are present when $\tau = 0$, but these will involve very high frequencies of order $1/\tau$. This becomes unphysical in the sense that by the time convection responds to the forcing, the forcing may have changed sign. In practice, we will not be concerned with these spurious very high-frequency modes, confining our attention to modes with time scales much longer than the convective time scale represented by τ. For these solutions, there are six roots of (20) of which at least three are disallowed by the boundary condition that v vanish at large y^2. (In some instances, more than three roots are forbidden.) Of the allowed roots, usually one or two represent growing modes.

Note that in all the solutions presented, the approximation

$$|\sigma\tau| \ll 1$$

is verified extremely well.

We find the roots of (20) by an iterative procedure in which a first guess is applied, the residual of (20) is found together with its derivatives with respect to the real and imaginary parts of the complex growth rate σ, and a new guess is made using these derivatives. The eigenvalues thus found may be considered accurate to within three significant figures. In addition, (20) can be reduced to second order in the case $n = -1$, representing the Kelvin-like modes. This can then be solved exactly and the solution compared with that found using the aforementioned procedure as a check of the latter. Solutions to (20) will be presented in section 3.

There is nothing in the WISHE mechanism that is intrinsic to the equatorial beta plane. It is also instructive to examine local solutions to (18) valid far from the equator. We can do this most easily by making a WKB approximation to the solution of (18) valid in the vicinity of a finite value of y; we accomplish this

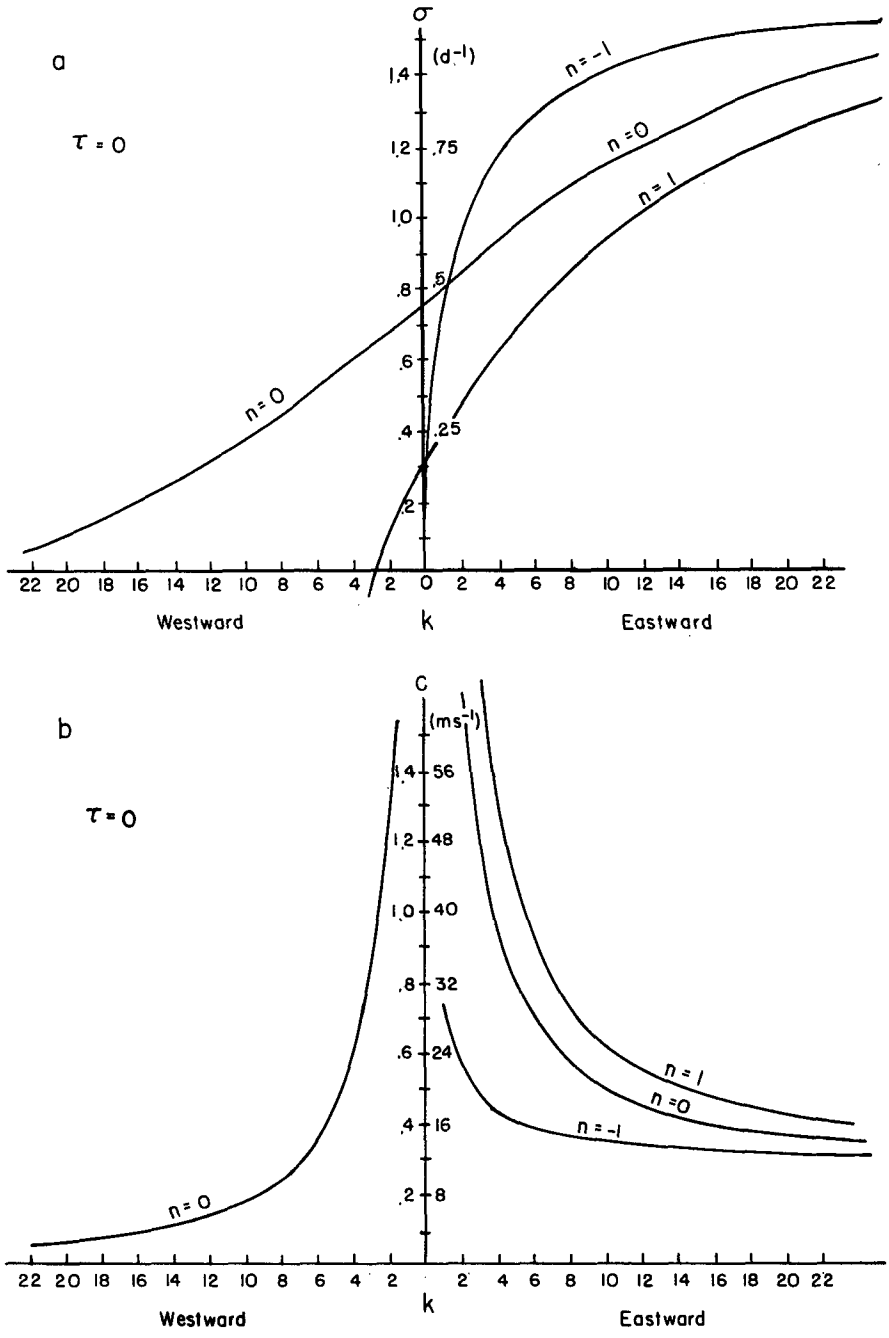

FIG. 1. (a) Growth rates and (b) phase speeds of the equatorial modes $n = -1$, $n = 0$, and $n = 1$ for zero convective response time (τ) and $P = 25$, $\epsilon_p = 0.9$. The nondimensional values are given at left and typical dimensional values at right.

by replacing y by y_0 in (18) and seeking modal solutions of the form

$$e^{ily},$$

where l is a meridional wavenumber. This is equivalent to phrasing the original equations on a middle-latitude beta plane, ignoring the meridional dependence of beta itself. Rather than seeking equatorially trapped solutions, we look for modes in the form of plane waves. It is also convenient to rescale the meridional coordinate y so that its scaling is the same as the scaling of x. This is accomplished by making the transformation

$$y \rightarrow \sqrt{P}y,$$

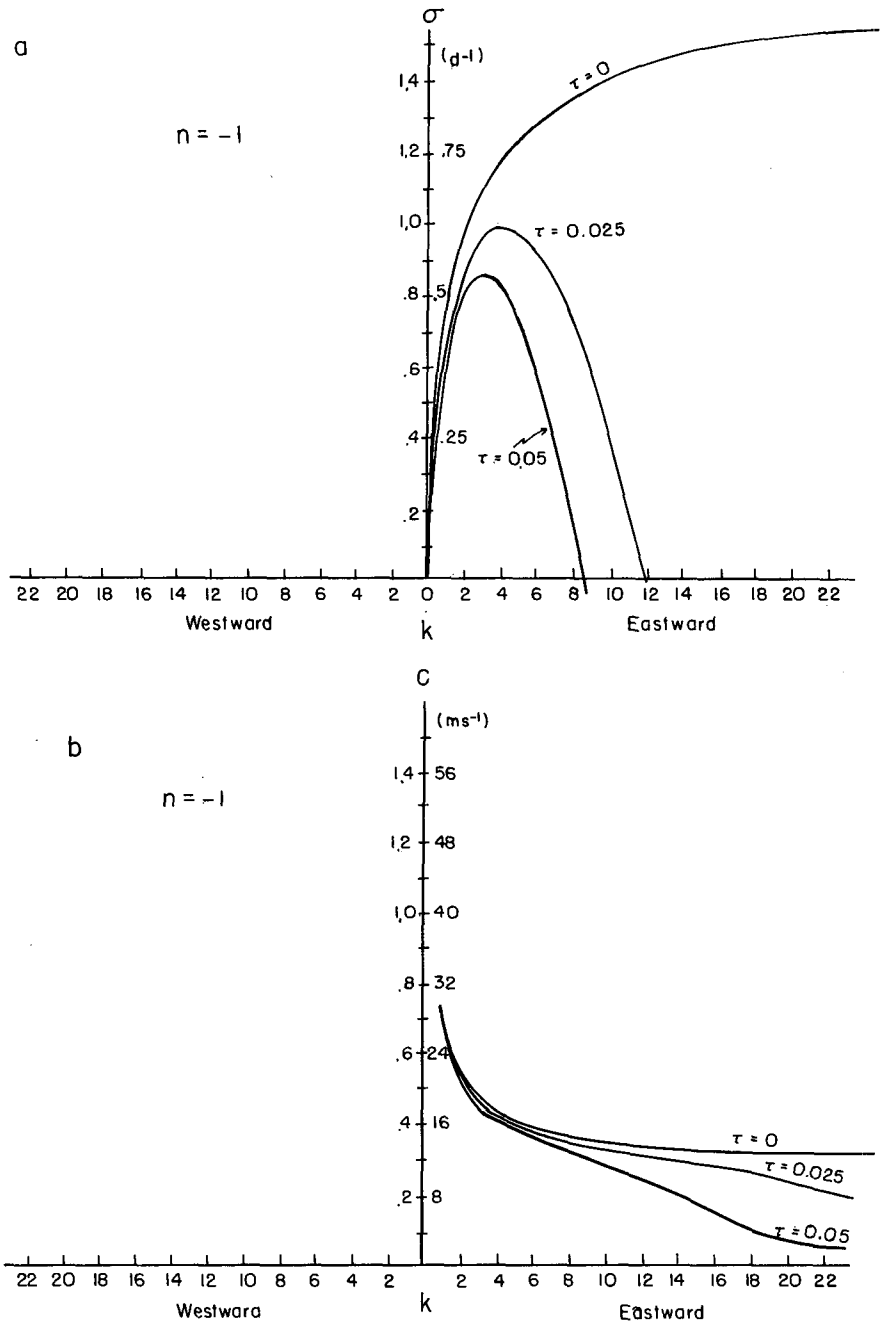

FIG. 2. As in Fig. 1 but for the $n = -1$ mode only, for three different values of the convective response time (τ).

where P is given by (17). The value of y_0 then gives the local value of the Coriolis parameter. With these substitutions, the first WKB eigenvalue relation from (18) is

$$\sigma^3 + \sigma(\chi(k^2 + l^2) + P^2 y_0^2 + ike^{-\sigma\tau}) + P(ily_0 e^{-\sigma\tau} + e^{-\sigma\tau} - ik\chi) = 0. \quad (21)$$

As we are interested in modes with time scales much longer than the cumulus adjustment time scale τ, we approximate the exponential terms in (21) by

$$e^{-\sigma\tau} \approx 1 - \sigma\tau.$$

For the solutions we will discuss, this is always an excellent approximation. Substituting this into (21) gives

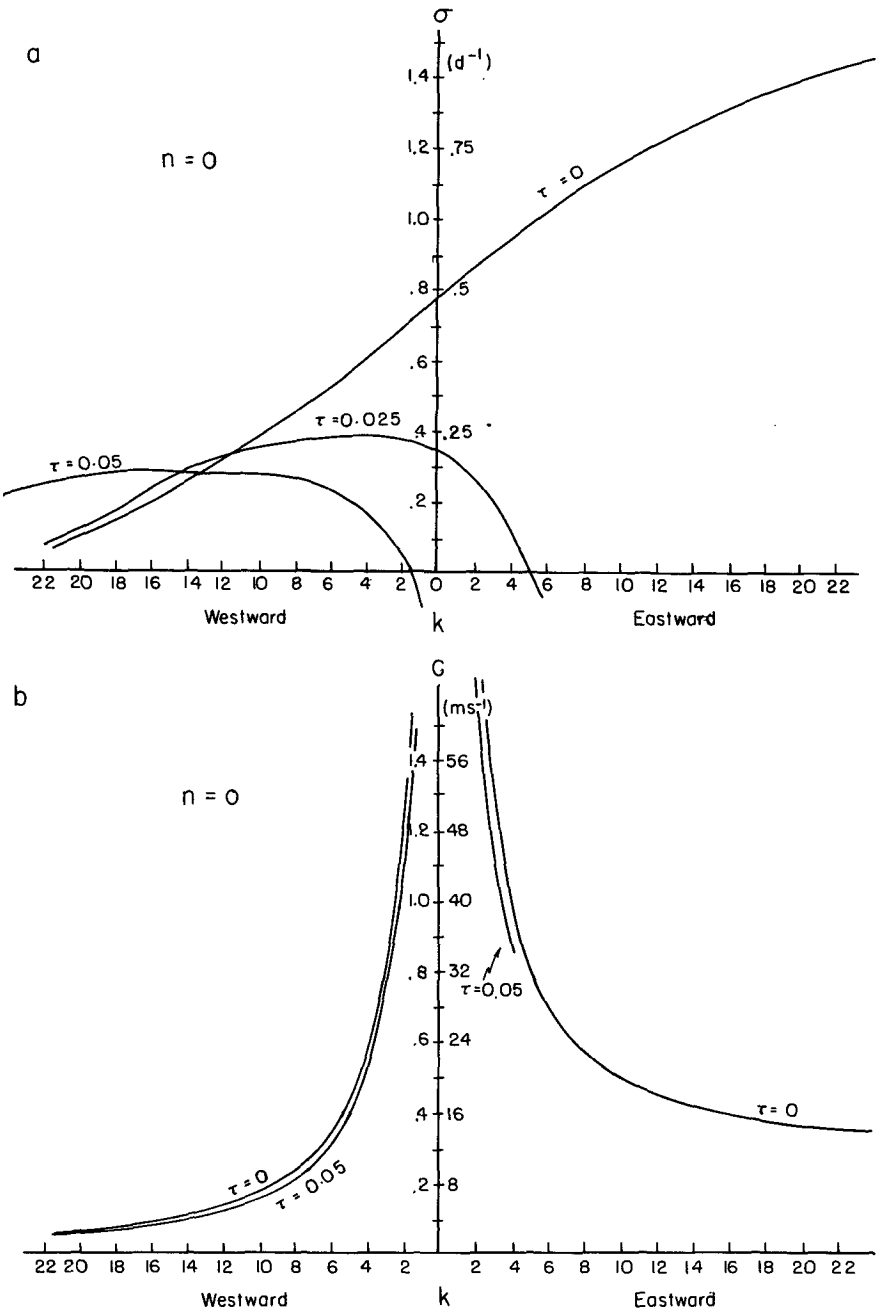

FIG. 3. As in Fig. 2 but for the $n = 0$ mode.

$$\sigma^3 + \sigma^2\tau[\epsilon_p(k^2 + l^2) - ik] + \sigma[(1 - \epsilon_p)(k^2 + l^2) + P^2y_0^2 + ik - P\tau(ily_0 + 1 + ik\epsilon_p)] + P[ily_0 + 1 + ik(1 - \epsilon_p)] = 0, \quad (22)$$

where we have made use of the definition of χ. This cubic equation is solved explicitly for the complex growth rate σ.

3. Solutions

We first examine solutions of the eigenvalue equation (20) pertaining to equatorially trapped modes. We consider only the modes corresponding to $n = -1$, $n = 0$, and $n = 1$ for reasons to be discussed presently. [Note that terminology such as "Kelvin wave" and "mixed Rossby–gravity wave" is avoided here because

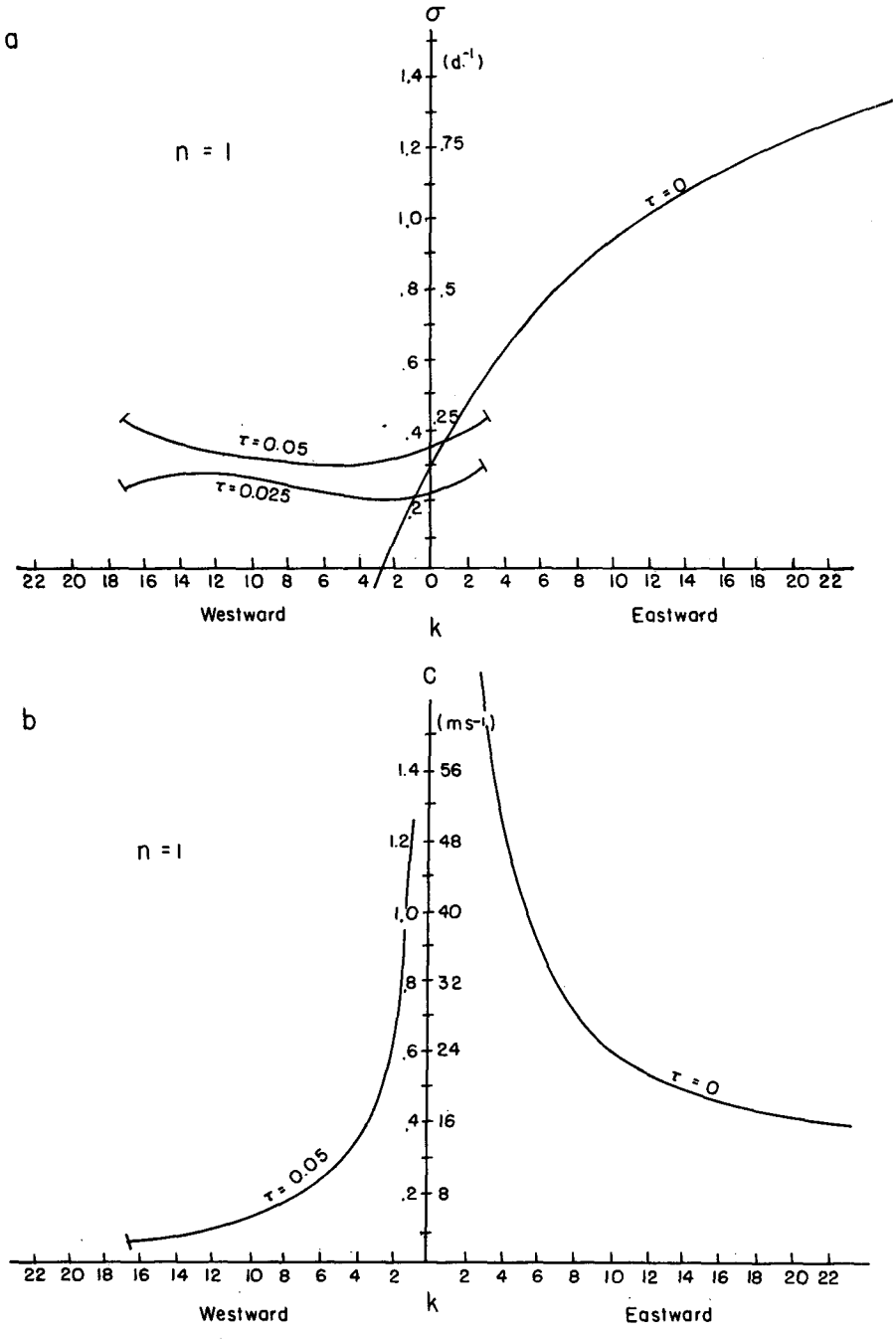

FIG. 4. As in Figs. 2 and 3 but for the $n = 1$ mode. (Phase speed curve for $\tau = 0.025$ indistinguishable from $\tau = 0.05$.)

such terminology can be misleading. As shown by Emanuel (1987), the WISHE mechanism itself gives rise to propagation even in the absence of potential vorticity gradients and gravitational stratification. For this reason, we will refer to the equatorially trapped modes only by their mode number, where it is understood that in the classical theory of stable equatorial waves $n = -1$ corresponds to the Kelvin wave, $n = 0$ to the mixed Rossby–gravity wave, and higher values of n to inertia–gravity waves.] In all cases, only one unstable branch for each value of n was found in a domain in which the zonal wavenumber k varies from minus to plus infinity, excluding the disallowed modes that do not decay at large y.

Figure 1 shows the growth rates and phase speeds of the first three modes, as functions of the zonal wavenumber, in the case that $\tau = 0$. These pertain to the case that $P = 25$ and $\epsilon_p = 0.9$, but it can be shown that when $\tau = 0$, ϵ can be absorbed in the scaling.[1] Thus, the curves in Fig. 1 can be considered to vary with P only. The $n = -1$ mode is the one proposed by Neelin et al. (1987) and Emanuel (1987) as possibly associated with the 30–50-day oscillation in the tropics; YE showed that when the troposphere is coupled to a stratosphere into which wave propagation is allowed, these modes have a short-wave cutoff and growth rates that peak at the planetary scale. There are no allowed westward-propagating solutions at $n = -1$.

The higher-order modes have generally smaller growth rates and higher frequencies. The $n = 0$ waves have a continuous spectrum of westward-propagating modes, but the waves that propagate eastward have higher growth rates. The $n = 1$ modes are strongly biased toward eastward propagation, though some weakly growing westward-propagating modes occur at planetary scales. All but the $n = -1$ modes have finite nonzero frequencies when $k = 0$.

Note that in no case is a growth rate peak observed at finite zonal wavenumber.

The effect of convective time lags on the $n = -1$ mode is shown in Fig. 2, which depicts the growth rates and phase speeds for two values of τ, corresponding dimensionally to about 1 and 2 h, respectively. (These also pertain to the case $P = 25$, and $\epsilon_p = 0.9$; when τ is nonzero, there are three independent dimensionless parameters instead of one.) The effects are dramatic. The higher-frequency modes are strongly damped, leaving only planetary-scale waves. Phase speeds are hardly affected in the range of k of growing modes. The effects are similar to those of coupling with the stratosphere (see YE), but quantitatively stronger for very modest response times.

Figures 3 and 4 show the effects of response time on the higher-order modes. The eastward-propagating component of the $n = 0$ wave is virtually eliminated, leaving westward-propagating modes over a broad range of zonal wavenumbers, from the planetary down to the synoptic scale, but phase speeds of these modes are hardly affected by convective response time. These phase speeds are very modest near the wavenumbers of peak growth. The intrinsic frequency of these modes is negative and decreases in magnitude with increasing wavenumber; thus, the group velocity of the $n = 0$ mode is eastward. The $n = 1$ mode exists only over a finite range of k when τ is positive; outside this range these modes are disallowed by the condition that their amplitude decay at large y^2. For these modes as well, the eastward-propagating components are virtually eliminated, and their growth rates are comparable to those of the $n = 0$ modes. Their phase speeds, however, are dramatically reduced by nonzero convective response times.

The spatial structure of the modes described here are in most respects very similar to their counterparts in the classical stable modes of the equatorial waveguide and to the solutions discussed by Neelin et al. (1987) and thus will not be dwelled upon here. We do note, however, that when n is one or larger, the modes have no amplitude on the equator and generally exhibit peak amplitudes in the subtropics and middle latitudes, where they generally have rapid meridional variation. For this reason, the WKB analysis of (18), resulting in the eigenvalue equation (22), seems particularly appropriate. [Recall that the y coordinate has been rescaled so that it has the same scale as the x coordinate (see Table 1). Also, the quantity $e^{-\sigma\tau}$ has been approximated by $1 - \sigma\tau$ (see section 2).]

The solutions of the cubic equation (22), pertaining to WISHE modes on a middle-latitude beta plane, exhibit two classes of growing modes: low-frequency eastward-propagating waves and high-frequency waves that always propagate poleward and may have eastward or westward components of propagation as well.

Figure 5 displays the growth rates and phase speeds of only the most rapidly growing mode over a particular range of zonal and meridional wavenumbers. These are for the case that the response time τ is zero, $P = 25$, $\epsilon_p = 0.9$, and $y_0 = 0.6$, the last corresponding to the value of the Coriolis parameter at about 40°N latitude. In this case, the eastward-propagating low-frequency mode has the highest growth rates. The growth rate asymptotes to the same value as does the equatorial $n = -1$ mode for very large k and $l = 0$, but for the finite range of k illustrated in Fig. 5, growth rates are higher at positive values of l. This shows that the most unstable modes at finite zonal wavenumber have a northwest–southeast tilt in the Northern Hemisphere; these are just the manifestations of the $n = -1$ equatorial mode, whose eigenfunctions tilt in the same direction at higher latitudes.

The growth rates and phase speeds of the westward-propagating unstable modes over a particular range of zonal and meridional wavenumber are shown in Fig. 6 for the same parameters as in Fig. 5. In this case there is a broad growth rate peak at a zonal wavenumber of about 50 and a meridional wavenumber near 40. These are poleward- and westward-propagating modes whose growth rates and phase speeds are much smaller than those of the eastward-moving wave. The dimensional

[1] Although the quantization of zonal wavenumber is lost, the transformations $u \to (1 - \epsilon_p)u$, $v \to (1 - \epsilon_p)^{1/4}v$, $T \to (1 - \epsilon_p)^{3/2}T$, $y \to (1 - \epsilon_p)^{1/4}y$, $k \to (1 - \epsilon_p)^{-1}k$, $D \to (1 - \epsilon_p)^{-1/2}D$, together with a redefinition of P, $P' \equiv P(1 - \epsilon_p)^{3/2}$, render (13)–(16) a function of the single nondimensional parameter P' when $\tau = 0$. Neither YE nor Goswami and Goswami (1991) seem to have recognized that their equations, without the damping terms, could be reduced to a one-parameter set.

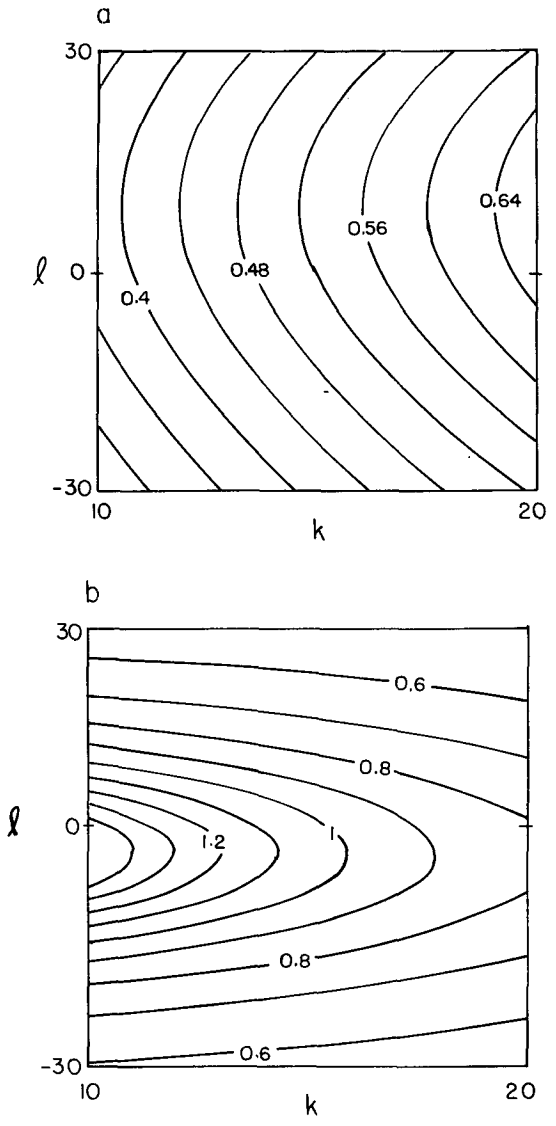

FIG. 5. Solutions of the WKB dispersion relation (22) on the mid-latitude beta plane. This shows the (a) dimensionless growth rate and (b) magnitude of the phase speed of the unstable eastward-propagating mode, in a particular region of the $k - l$ wavenumber plane, for zero convective response time (τ) and for $P = 25$, $\epsilon_p = 0.9$, and $y_0 = 0.6$. Note that in this analysis the y coordinate has been rescaled to have the same scale as the x coordinate in Table 1.

wavelength of the most rapidly growing mode is about 1000 km, and the phase speed relative to the flow is only about 1 m s^{-1}. The growth rate is, however, much smaller than the damping terms omitted in this analysis, so that it is unlikely that these would be observed.

Once again, the effect of small convective response times is dramatic, as illustrated in Figs. 7 and 8. As in the case of the equatorially trapped modes, all but the longest eastward-propagating modes are damped and the most unstable mode has growth rates of the same order as the omitted damping terms. In this case, a center of very high growth rates occurs at small, negative meridional wavenumbers, indicating equatorward and eastward propagation. But these modes have frequencies that are extremely small, of order one-half day, and thus violate the assumption that the wave periods are much longer than the convective response time. These solutions are therefore unphysical and should be discarded.

As shown in Fig. 7, however, the poleward- and westward-propagating disturbances are enhanced by small convective response times, achieving growth rates comparable to expected damping rates. Moreover, this

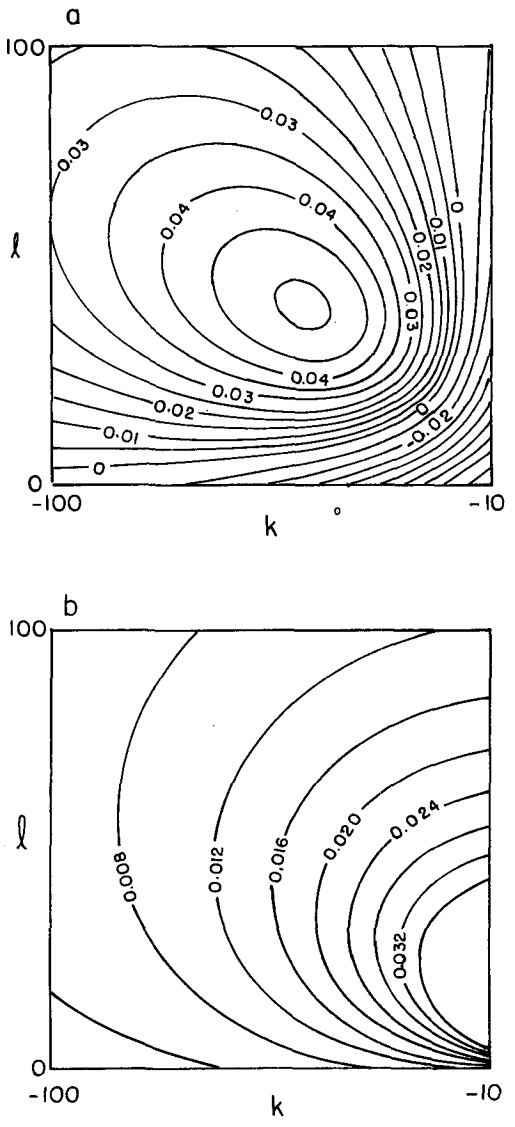

FIG. 6. As in Fig. 5 but showing the unstable westward-propagating branch over a portion of $k - l$ wavenumber space. Note different ranges of k and l.

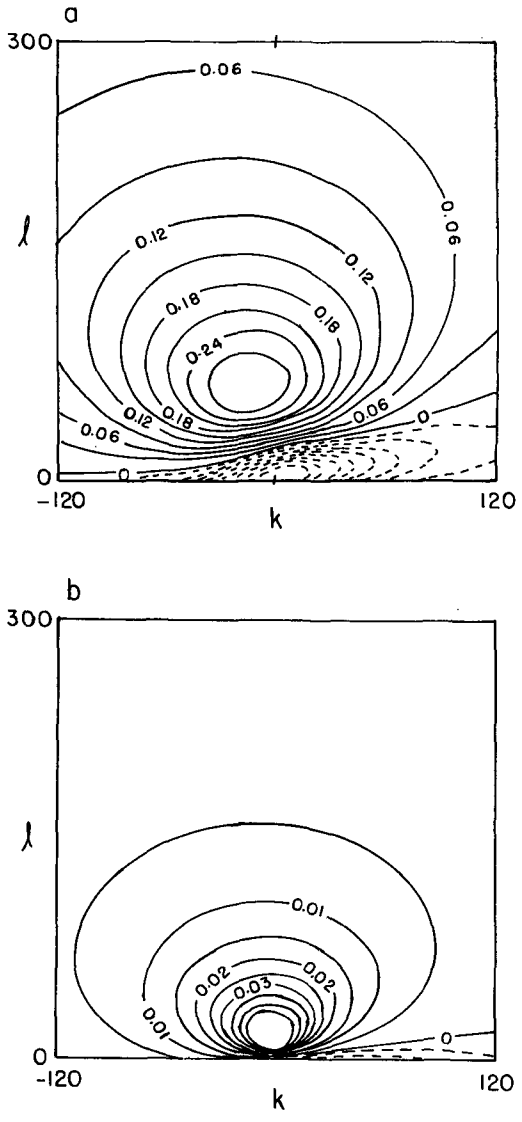

FIG. 7. As in Fig. 5 but for convective response time (τ) of 0.025. An unstable root highly localized in the region of small k has been omitted; see Fig. 8. Phase propagation is poleward; westward for negative k and eastward for positive k. Note different ranges of k and l.

branch of unstable modes now extends into the eastward-propagating sector. All of these modes, which include zonally symmetric modes, propagate poleward. Flow-relative phase speeds are of the order of 1 m s^{-1} and wavelengths are still of order 1000 km. The group velocities of these modes (not shown) vary considerably over the range of scales shown in Fig. 7, but near the wavelengths of maximum growth the wave energy propagates very slowly southeastward for the parameters used in Fig. 7. For all practical purposes, the wave energy associated with the poleward- and westward-propagating modes travels with the mean wind.

4. Discussion

The WISHE mechanism, by tapping the very large reservoir of energy associated with the thermodynamic disequilibrium between the tropical oceans and atmosphere, offers a promising explanation for a variety of tropical disturbances. Besides hurricanes, which certainly operate on this mechanism, phenomena as diverse as the 40–50-day oscillation and westward-moving synoptic-scale disturbances may owe their existence to WISHE. Here we have shown that linear WISHE modes are sensitive to the time it takes convection to respond to the large scale, even though this time may be very small compared to the time scales

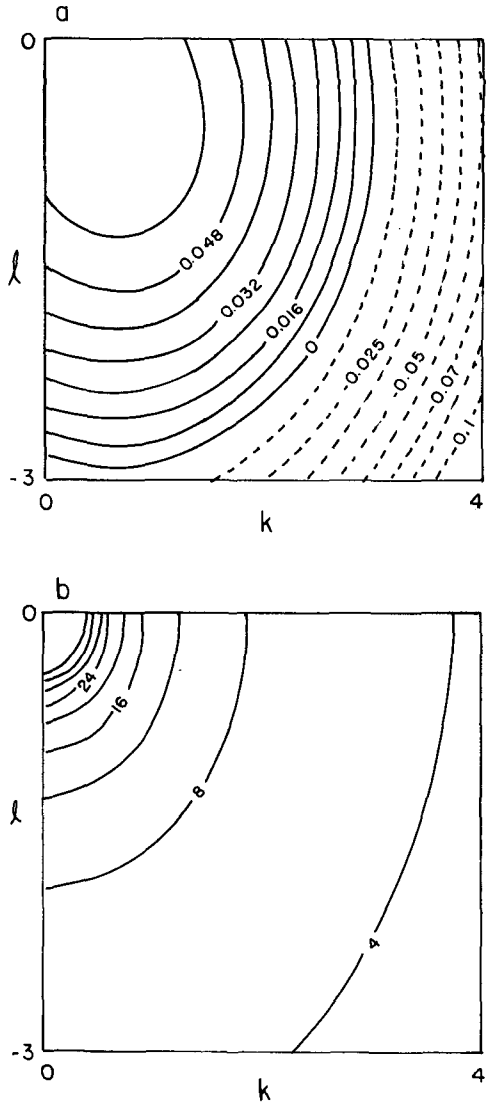

FIG. 8. As in Fig. 7 but showing the other unstable root. Note different ranges of k and l.

of the disturbances in question. Though quasi equilibrium may be almost exact in the tropics, the very small disequilibrium between convection and the large-scale processes that sustain it has a large effect on tropical disturbances, according to the present analysis.

It is not difficult to understand why this is so. In the conceptual and physical framework developed by Neelin et al. (1987), Emanuel (1987), and YE, the dominant effects on the frequency of linear tropical waves are the gradient of potential vorticity (beta) and the effective stratification of the tropical troposphere to deep perturbations, which is positive even when convection is accounted for, because the downdrafts associated with convection cause a reduction of the entropy of the subcloud layer and hence of the temperature of the free atmosphere, which is held close to a neutral state by convection. Even the reduced effective stratification, however, is a strong influence on wave frequencies.

The growth of unstable waves, on the other hand, is controlled by the comparatively small variations in atmospheric temperature that result from variations in the surface enthalpy flux coupled with convective redistribution of heat. The phase relationships of these fluxes to the waves' temperature perturbations give rise to both growth (or decay) and propagation, as a general rule, although the latter effect is usually small compared to the aforementioned effects.

In a state of perfect statistical equilibrium, the convection induced by large-scale ascent in waves is exactly out of phase with the temperature perturbations associated with the waves. This affects their rate of propagation, but does not contribute to growth or decay. When the convection lags behind the forcing by even a small amount, however, its occurrence is biased slightly toward the regions of negative temperature perturbations. The resulting negative correlation between temperature and heating is a negative effect on the wave growth. Clearly, the magnitude of this effect depends on the relative magnitudes of the response time of the convection and the period of the wave. The damping is particularly strong when the wave period is short. As the frequencies of WISHE modes tend to be larger than their growth rates, the damping effect of small convective response times can be large compared to quasi-equilibrium growth rates.

Although the phase lag acting on the component of convection forced by large-scale ascent always acts to damp the waves (at least in barotropic environments), the phase lag acting on convection forced by surface enthalpy flux anomalies may in some circumstances act to increase the growth of the waves. This is especially true for the lower-frequency westward-propagating waves, whose growth is enhanced by nonzero convective response times, both in the case of equatorially trapped waves and waves on a middle-latitude beta plane.

The net result of including a small convective response time is to favor the following WISHE modes in a background of constant easterly flow:

1) Kelvin-like, ($n = -1$) eastward-propagating equatorially trapped waves of small zonal wavenumber. The phase speed of such waves is sensitive to the assumed precipitation efficiency of convection, but values in the range 10–20 m s^{-1} are typical. These were proposed as explanations of the 30–50-day oscillation in the equatorial zone by Neelin et al. (1987) and Emanuel (1987).

2) Westward-propagating equatorially trapped $n = 0$ modes similar to mixed Rossby gravity waves. Depending on the convective response time, these are unstable over a broad frequency and zonal wavenumber range. In dimensional terms, wavelengths in the range of 2000 to 10 000 km and flow-relative periods of 5–10 days (3–7 days for an observer fixed with respect to the earth) are indicated. Goswami and Goswami (1991) suggested that such modes might be associated with various observed westward-moving disturbances in the tropics.[2] The time and space scales of these WISHE modes, their spatial structure, westward phase speed, and eastward group velocity are all in accord with the observational analysis of Liebmann and Hendon (1990).

3) A variety of poleward-propagating synoptic-scale (1000-km) disturbances not necessarily trapped around the equator. There is a preference for westward propagation, although eastward-propagating modes and zonally symmetric modes occur as well. Flow-relative phase speeds and group velocities are very small (0.5–1 m s^{-1}), so that these disturbances may be considered to move approximately with the mean flow. As typical growth rates are not much larger than expected damping time scales (the linear damping terms have been omitted in the present analysis), the WISHE mechanism may play a greater role in sustaining, or slowing the decay of, disturbances generated by other mechanisms. WISHE may, for example, sustain easterly waves generated over Africa as they move westward over the Atlantic.

The results presented here suggest that strong distortions of tropical wave activity may occur in numerical models in which the quasi equilibrium of convection is rigorously enforced, as in models using the convection scheme of Arakawa and Schubert (1974).

Unfortunately, it is difficult to devise field experiments or uses of previously obtained experimental datasets that are capable of rejecting most of the extant

[2] Goswami and Goswami (1991) reported growth rate peaks at finite zonal wavenumber for the $n = 0$ mode with no convective lag. This result is not confirmed here, at least for the value of P used in this analysis.

hypotheses on the formation and maintenance of tropical wave disturbances. Part of the problem is that the virtual temperature perturbations associated with such waves are too small to be observed directly with any accuracy. For disturbances whose flow-relative frequencies are smaller than the local value of the Coriolis parameter, including virtually all the easterly waves discussed in the literature, the density fluctuations could in principle be derived from the observed wind field, provided the observations are of sufficient accuracy and extent. This would be a major step toward testing the various theories proposed to explain the waves.

Testing the WISHE hypothesis against CISK poses its own difficulties. In both theories, convection is almost entirely in phase with the large-scale vertical motion; the phase shift due to surface flux anomalies that is responsible for growth in the WISHE framework is probably too slight to be observed. A conclusive test would be to determine the relative phase of free atmosphere virtual temperature perturbations and subcloud-layer entropy anomalies; in CISK these would be negatively correlated while in WISHE they would be correlated positively. Unfortunately, the accuracy of subcloud-layer humidity measurements is probably too small, since a one-degree free atmospheric temperature perturbation is associated with a subcloud-layer relative humidity fluctuation of only about 1% or 2%. Time series of very high quality temperature and moisture soundings in regions experiencing the wave disturbances might provide an adequate test.

Acknowledgments. This research is supported by Grant 9103025-ATM from the National Science Foundation. The research was conducted while the author was in residence at Meteo France, which he thanks for its support.

REFERENCES

Arakawa, A., and W. H. Schubert, 1974: Interaction of a cumulus cloud ensemble with the large-scale environment. Part I. *J. Atmos. Sci.*, **31**, 674–701.

Betts, A. K., 1982: Saturation point analysis of moist convective overturning. *J. Atmos. Sci.*, **39**, 1484–1505.

——, and M. J. Miller, 1986: A new convective adjustment scheme. Part II. *Quart. J. Roy. Meteor. Soc.*, **112**, 693–709.

Charney, J. G., and A. Eliassen, 1964: On the growth of the hurricane depression. *J. Atmos. Sci.*, **21**, 68–75.

Emanuel, K. A., 1986: An air–sea interaction theory for tropical cyclones. Part I. *J. Atmos. Sci.*, **43**, 585–604.

——, 1987: An air–sea interaction model of intraseasonal oscillations in the tropics. *J. Atmos. Sci.*, **44**, 2324–2340.

——, 1989: The finite-amplitude nature of tropical cyclogenesis. *J. Atmos. Sci.*, **46**, 3431–3456.

Goswami, P., and B. N. Goswami, 1991: Modification of $n = 0$ equatorial waves due to interaction between convection and dynamics. *J. Atmos. Sci.*, **48**, 2231–2244.

Kleinschmidt, E., Jr., 1951: Gundlagen einer Theorie des tropischen Zyklonen. *Archiv. Meteorol., Geophys. Bioklim.* Ser. A, **4**, 53–72.

Liebmann, B., and H. H. Hendon, 1990: Synoptic-scale disturbances near the equator. *J. Atmos. Sci.*, **47**, 1463–1479.

Neelin, J. D., I. M. Held, and K. H. Cook, 1987: Evaporation–wind feedback and low-frequency variability in the tropical atmosphere. *J. Atmos. Sci.*, **44**, 2341–2348.

Ooyama, K., 1964: A dynamical model for the study of tropical cyclone development. *Geofis. Int.*, **4**, 187–198.

Randall, D. A., and J. Wang, 1992: The moist available energy of a conditionally unstable atmosphere. *J. Atmos. Sci.*, **49**, 240–255.

Xu, K., and K. A. Emanuel, 1989: Is the tropical atmosphere conditionally unstable? *Mon. Wea. Rev.*, **117**, 1471–1479.

Yano, J., and K. A. Emanuel, 1991: An improved model of the equatorial troposphere and its coupling with the stratosphere. *J. Atmos. Sci.*, **48**, 377–389.